HAL
open science

Estimates of phytoplankton class-specific and total primary production in the Mediterranean Sea from satellite ocean color observations

Julia Uitz, Dariusz Stramski, Bernard Gentili, Fabrizio d'Ortenzio, Hervé Claustre

To cite this version:

Julia Uitz, Dariusz Stramski, Bernard Gentili, Fabrizio d'Ortenzio, Hervé Claustre. Estimates of phytoplankton class-specific and total primary production in the Mediterranean Sea from satellite ocean color observations. Global Biogeochemical Cycles, 2012, 26 (2), pp.n/a-n/a. 10.1029/2011GB004055 . hal-03137464

HAL Id: hal-03137464

https://hal.science/hal-03137464v1

Submitted on 10 Feb 2021

HAL is a multi-disciplinary open access archive for the deposit and dissemination of scientific research documents, whether they are published or not. The documents may come from teaching and research institutions in France or abroad, or from public or private research centers.

L'archive ouverte pluridisciplinaire **HAL**, est destinée au dépôt et à la diffusion de documents scientifiques de niveau recherche, publiés ou non, émanant des établissements d'enseignement et de recherche français ou étrangers, des laboratoires publics ou privés.

Estimates of phytoplankton class-specific and total primary production in the Mediterranean Sea from satellite ocean color observations

Julia Uitz,[1,2,3] Dariusz Stramski,[1] Bernard Gentili,[4,5] Fabrizio D'Ortenzio,[4,5] and Hervé Claustre[4,5]

Received 9 February 2011; revised 2 March 2012; accepted 6 April 2012; published 24 May 2012.

[1] An approach that combines a recently developed procedure for improved estimation of surface chlorophyll *a* concentration (Chl_{surf}) from ocean color and a phytoplankton class-specific bio-optical model was used to examine primary production in the Mediterranean Sea. Specifically, this approach was applied to the 10 year time series of satellite Chl_{surf} data from the Sea-viewing Wide Field-of-view Sensor. We estimated the primary production associated with three major phytoplankton classes (micro, nano, and picophytoplankton), which also yielded new estimates of the total primary production (P_{tot}). These estimates of P_{tot} (e.g., 68 g C m^{-2} yr^{-1} for the entire Mediterranean basin) are lower by a factor of ~2 and show a different seasonal cycle when compared with results from conventional approaches based on standard ocean color chlorophyll algorithm and a non-class-specific primary production model. Nanophytoplankton are found to be dominant contributors to P_{tot} (43–50%) throughout the year and entire basin. Micro and picophytoplankton exhibit variable contributions to P_{tot} depending on the season and ecological regime. In the most oligotrophic regime, these contributions are relatively stable all year long with picophytoplankton (~32%) playing a larger role than microphytoplankton (~22%). In the blooming regime, picophytoplankton dominate over microphytoplankton most of the year, except during the spring bloom when microphytoplankton (27–38%) are considerably more important than picophytoplankton (20–27%).

Citation: Uitz, J., D. Stramski, B. Gentili, F. D'Ortenzio, and H. Claustre (2012), Estimates of phytoplankton class-specific and total primary production in the Mediterranean Sea from satellite ocean color observations, *Global Biogeochem. Cycles*, *26*, GB2024, doi:10.1029/2011GB004055.

1. Introduction

[2] Often considered as a small-scale model of the world ocean [*Bethoux et al.*, 1999] and identified as one of the most sensitive regions to climate change [*Giorgi*, 2006], the Mediterranean Sea is of particular interest for biogeochemical studies [*The MerMex Group*, 2011]. Several investigators have used satellite ocean color data in conjunction with bio-optical models to assess primary production in various regions of the Mediterranean [e.g., *Morel and André*, 1991; *Antoine et al.*, 1995; *Bosc et al.*, 2004; *Lazzara et al.*, 2010]. The present study is motivated by recent advancements in the field of bio-optical modeling and remote sensing estimation of chlorophyll *a* concentration (Chl) in the surface ocean, which is a key input parameter to bio-optical primary production models.

[3] Standard ocean color algorithms have been shown to significantly overestimate the surface Chl (Chl_{surf}) in Mediterranean waters [*Bricaud et al.*, 2002; *Claustre et al.*, 2002; *Gregg and Casey*, 2004]. This led to the development of numerous regional algorithms whose validity is inherently limited by the data set from which the algorithms were established [*Bricaud et al.*, 2002; *D'Ortenzio et al.*, 2002; *Volpe et al.*, 2007]. Using a recently developed approach [*Morel and Gentili*, 2009a], *Morel and Gentili* [2009b] demonstrated that the overestimation of ocean color–derived Chl_{surf} in the Mediterranean from traditional

[1]Marine Physical Laboratory, Scripps Institution of Oceanography, University of California, San Diego, La Jolla, California, USA.
[2]Now at Laboratoire d'Océanographie de Villefranche, Unité Mixte de Recherche 7093, Université Pierre et Marie Curie, Villefranche-sur-Mer, France.
[3]Now at Laboratoire d'Océanographie de Villefranche, Unité Mixte de Recherche 7093, Centre National de la Recherche Scientifique, Villefranche-sur-Mer, France.
[4]Laboratoire d'Océanographie de Villefranche, Unité Mixte de Recherche 7093, Université Pierre et Marie Curie, Villefranche-sur-Mer, France.
[5]Laboratoire d'Océanographie de Villefranche, Unité Mixte de Recherche 7093, Centre National de la Recherche Scientifique, Villefranche-sur-Mer, France.

Corresponding author: J. Uitz, Laboratoire d'Océanographie de Villefranche, Port de la Darse, BP 8, F-06238 Villefranche-sur-Mer CEDEX, France. (julia.uitz@obs-vlfr.fr)

Copyright 2012 by the American Geophysical Union.
0886-6236/12/2011GB004055

algorithms is caused by generally higher concentrations of colored dissolved organic matter (CDOM) in these waters compared with the average CDOM expected on the basis of actual local Chl_{surf} levels. This approach provides a means for correcting ocean color Chl_{surf} data, which results in more realistic lower values of satellite-derived Chl_{surf} and a modified seasonal cycle of this data product [*Morel and Gentili*, 2009b]. Such changes in the estimation of Chl_{surf} are expected to impact substantially the ocean color-based estimates of primary production.

[4] Several algorithms were recently developed for discriminating major phytoplankton types from ocean color observations (see review by *Nair et al.* [2008] and *Brewin et al.* [2011]). Specifically, a novel approach was proposed for quantifying the chlorophyll *a* biomass [*Uitz et al.*, 2006] and primary production [*Uitz et al.*, 2008] associated with three phytoplankton classes, i.e., microphytoplankton (typically dominated by diatoms), nanophytoplankton (e.g., prymnesiophytes), and picophytoplankton (e.g., cyanobacteria). *Uitz et al.* [2010] present an application of this approach for estimating phytoplankton class-specific primary production at the global scale. This approach provides insights into the spatial and temporal patterns of succession of phytoplankton types with subsequent impact on carbon fluxes.

[5] By combining the satellite ocean color data from Seaviewing Wide Field-of-view Sensor (SeaWiFS) with the above mentioned recent advancements, we can reassess the estimates of total primary production and propose the first estimates of phytoplankton class-specific primary production in the Mediterranean Sea. For this purpose, we applied the class-specific approach of *Uitz et al.* [2006, 2008] to the 10 year time series of SeaWiFS-derived Chl_{surf} data corrected for CDOM according to *Morel and Gentili* [2009a]. Our analysis is focused on the mean seasonal cycle of the total and class-specific primary production within several ecological regimes (referred to as clusters) defined by *D'Ortenzio and Ribera d'Alcalà* [2009]. We also compare these results with those obtained from uncorrected satellite values of Chl_{surf} and a standard (non-class-specific) version of the primary production model, as well as with some field measurements from the literature.

2. Data and Methods

[6] Satellite-based estimates of phytoplankton class-specific and total primary production were computed using the bio-optical primary production model of *Morel* [1991]. The satellite-derived Chl_{surf}, surface value of photosynthetically available radiation (PAR), and phytoplankton class-specific vertical profiles of chlorophyll *a* concentrations and photophysiological properties are required as input data.

[7] Level 3 monthly SeaWiFS data of Chl_{surf} (available from the NASA Ocean Biology Processing Group, 2009, http://oceancolor.gsfc.nasa.gov/REPROCESSING/R2009) and surface PAR were acquired from the NASA Ocean Color website for the period from January 1998 through December 2007 over the Mediterranean basin. The Chl_{surf} data are obtained from the OC4 algorithm [*O'Reilly et al.*, 2000] with modifications included in R2009. These data were then corrected for the "excess" of CDOM following the method described by *Morel and Gentili* [2009a, 2009b]. This method utilizes two band ratios of the spectral reflectance of the ocean, $R(\lambda)$, specifically $R(412)/R(443)$ and $R(490)/R(555)$, which are derived from SeaWiFS imagery. We consider exclusively the data of Chl_{surf} and PAR from noncoastal waters (i.e., ocean depths > 200 m) because the phytoplankton class-specific approach is based on open ocean data exclusively and is therefore applicable only to such environments [*Uitz et al.*, 2006, 2008].

[8] *Uitz et al.* [2006] developed a method for deriving vertical profiles of Chl associated with micro, nano, and picophytoplankton, using Chl_{surf} as input data. This method was developed through the statistical analysis of an extensive phytoplankton pigment database obtained from high-performance liquid chromatography (HPLC) analysis of samples from a variety of oceanic regions. The respective contributions of the three size-dependent classes to the total algal biomass in the database were obtained from a modified version of the diagnostic pigment criteria of *Vidussi et al.* [2001]. This method assigns seven diagnostic pigments to specific phytoplankton taxa which are categorized into three different pigment-based classes, which in turn are assumed to correspond approximately to the three size classes of the algal cells. As already emphasized in the past [*Vidussi et al.*, 2001; *Uitz et al.*, 2006], this pigment-based approach does not strictly reflect the true size structure of the phytoplankton assemblage because some diagnostic pigments may be shared by various taxonomic groups and some groups may have a wide range of cell size. Nevertheless, in spite of some limitations, this approach enables characterizing the taxonomic composition of the entire phytoplankton assemblage while simultaneously yielding reasonable information on its size structure [*Bricaud et al.*, 2004; *Uitz et al.*, 2009]. This is because microphytoplankton generally comprise mainly diatoms, nanophytoplankton prymnesiophytes, and picophytoplankton prokaryotes. For the sake of simplicity, thereafter we use the size-based terms micro, nano, and picophytoplankton for the three pigment-based phytoplankton classes as determined with the method of *Uitz et al.* [2006].

[9] To compute the vertical profiles of Chl associated with the three phytoplankton classes we use the CDOM-corrected Chl_{surf} data and the mixed layer depths obtained from the Mediterranean monthly climatology of *D'Ortenzio et al.* [2005] as input to the parameterization of *Uitz et al.* [2006]. The resulting class-specific Chl profiles and PAR data were then used in conjunction with the vertical profiles of class-specific photophysiological properties of *Uitz et al.* [2008] in the bio-optical primary production model of *Morel* [1991]. In brief, *Uitz et al.* [2008] investigated relationships between phytoplankton photophysiology and community composition by analyzing a large database of HPLC pigment determinations, measurements of phytoplankton absorption spectra, and photosynthesis-irradiance curve parameters. These data were collected from various temperate, subtropical, and tropical open ocean regions including the western and eastern Mediterranean basins. On the basis of these data an empirical model was proposed, which describes the dependence of algal photophysiology on the community composition and depth within the water column, essentially reflecting photoacclimation. The application of the model to the database from in situ observations enabled the identification of vertical profiles of photophysiological properties for each phytoplankton pigment-based size class. The

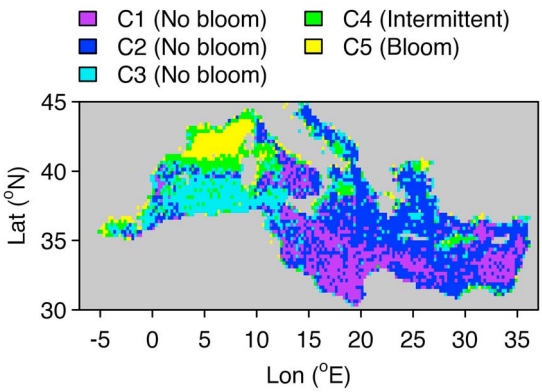

Figure 1. Geographic distribution of the five regional clusters considered in this study. The clusters are defined according to *D'Ortenzio and Ribera d'Alcalà* [2009].

photophysiological parameters required to run the *Morel* [1991] model were computed from these profiles.

[10] The calculations with the above approach provided vertical profiles of class-specific primary production rates. The estimates of water column–integrated primary production associated with microphytoplankton (P_{micro}), nanophytoplankton (P_{nano}), and picophytoplankton (P_{pico}) were then obtained by integrating the class-specific vertical profiles over the productive layer. The depth of this layer is defined as 1.5 times the depth of the euphotic layer which is limited by the 1% level of surface PAR. Finally, the total water column–integrated primary production (P_{tot}) was calculated as a sum of the contributions by the three phytoplankton classes, P_{micro}, P_{nano}, and P_{pico}. The reader is referred to *Uitz et al.* [2006, 2008] for full methodological details on the phytoplankton class-specific approach.

[11] In this study, this newly developed version of the model, which combines the CDOM-corrected Chl_{surf} data and the phytoplankton class-specific approach, is referred to as the v1 model. For comparison purposes, we use two additional versions of the model. The v2 model utilizes the standard SeaWiFS Chl_{surf} data in combination with the phytoplankton class-specific approach. The v3 model also utilizes the standard Chl_{surf} data, but with the standard (non-class-specific) approach of the model [*Antoine and Morel*, 1996]. In the v3 model, the assimilation number (P^B_{max}) varies with temperature as in *Eppley* [1972]. Sea surface temperature data required as input to v3 were taken from monthly AVHRR (Advanced Very High Resolution Radiometer) imagery.

[12] Regionalization is addressed by using five (out of the seven) clusters that were proposed by *D'Ortenzio and Ribera d'Alcalà* [2009] on the basis of the analysis of time series of uncorrected SeaWiFS Chl_{surf} data. This approach provides a general view of the different ecological regimes in the Mediterranean basin. The geographic distribution of the clusters is shown in Figure 1. The clusters C1, C2, and C3 reflect nonblooming waters covering a large part of the Mediterranean basin. The cluster C1 extends essentially south of 35°N and also covers most of the Tyrrhenian basin. The cluster C2 covers the Aegean, Adriatic, and central Ionian basins, and the cluster C3 the Algerian basin. The cluster C4 represents intermittently blooming waters, which include several areas scattered over the whole basin (the southern part of the Adriatic Gyre, the area off the northwestern Ionian coast, the Rhodes Gyre, the western Tyrrhenian basin, the Balearic front, the Liguro-Provençal current, and the Alboran Sea). The cluster C5 covers the northwestern part of the Mediterranean basin, where a prominent spring bloom occurs annually. The coastal clusters C6 and C7 are not considered in our analysis as the class-specific approach has been developed for noncoastal

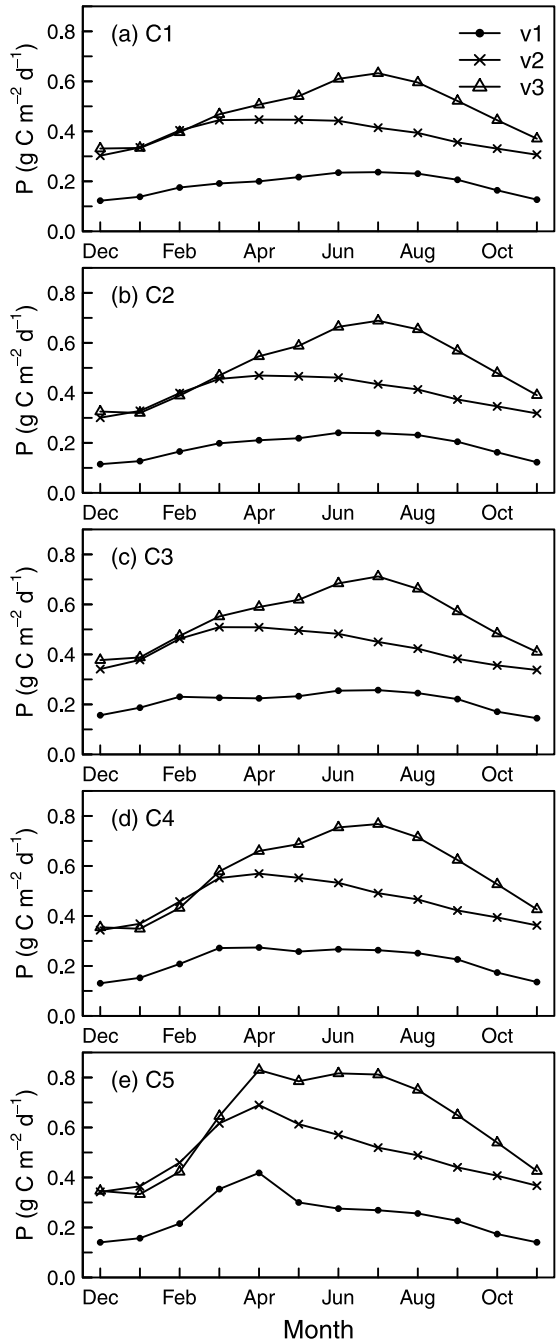

Figure 2. (a–e) Climatological mean (1998–2007) seasonal cycle of total primary production computed with the three different versions of the primary production model (v1, v2, and v3) for the five clusters under consideration (C1–C5) as indicated.

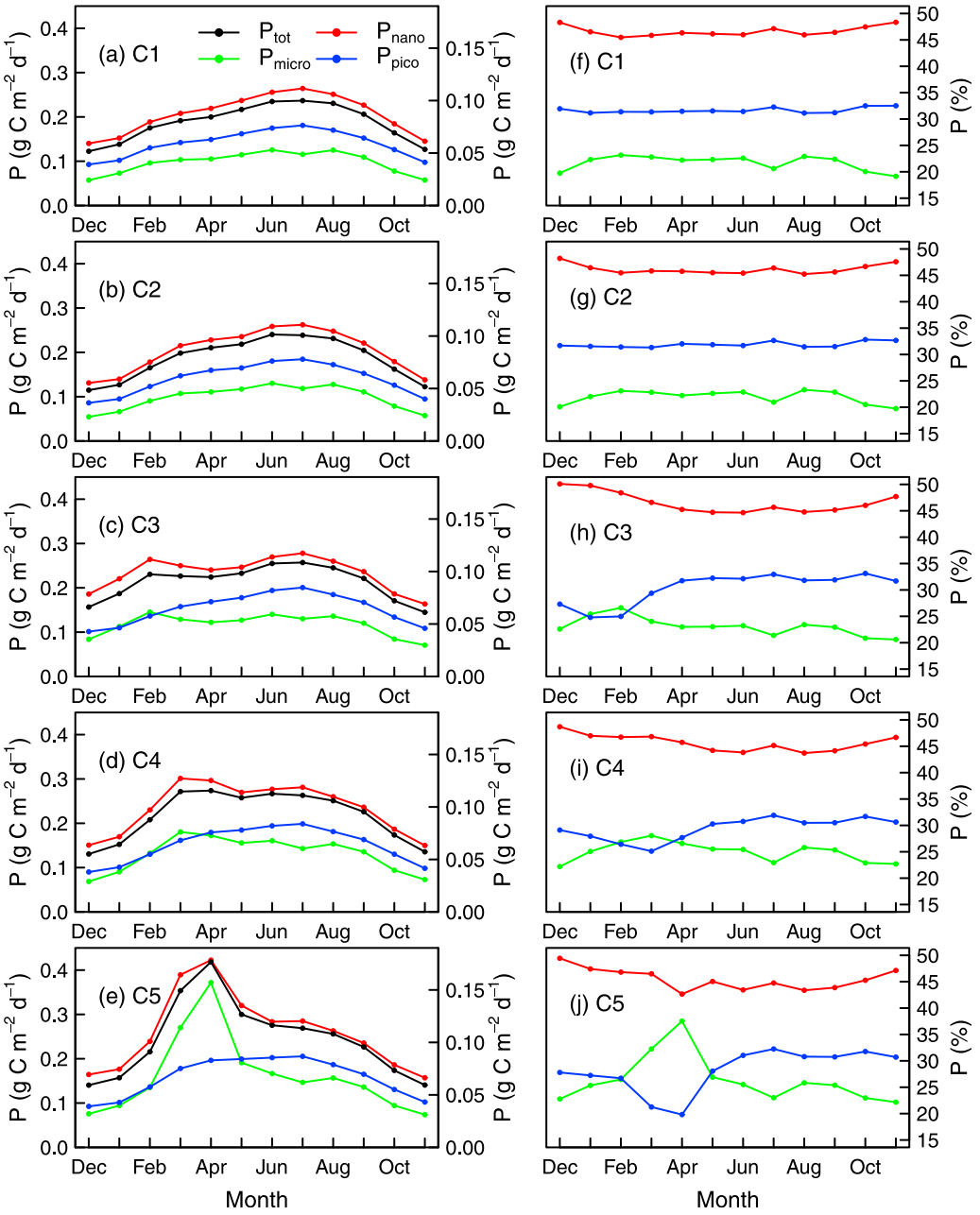

Figure 3. Climatological mean (1998–2007) seasonal cycle of total and class-specific primary production obtained from the v1 model for the five clusters under consideration (C1–C5) as indicated. Results are presented as absolute primary production rates (in units of g C m^{-2} d^{-1}) for (a–e) total and class-specific primary production, and (f–j) as a percent contribution of class-specific primary production to total primary production. Note the two different axes for absolute primary production rates; the left axis is for the total primary production and the right axis is for the class-specific primary production. The climatological seasonal cycle of the total primary production is reproduced from Figure 2.

(case 1) waters. Note that we also tested the cluster analysis of *D'Ortenzio and Ribera d'Alcalà* [2009] on the satellite-derived time series of Chl_{surf} corrected for CDOM and observed no significant differences in the resulting clusters.

[13] The mean seasonal cycles of P_{tot}, P_{micro}, P_{nano}, and P_{pico} were obtained by averaging the monthly values of each month over the 10 year time series for each cluster separately. The annual climatology calculated for the entire Mediterranean basin reflects the average of monthly mean values of P_{tot}, P_{micro}, P_{nano}, or P_{pico} over the full time series on a pixel-by-pixel basis.

[14] As a preliminary validation of our primary production estimates we compare the v1-derived annual estimates of P_{tot} with previously published estimates of P_{tot} obtained from field measurements. Whereas a number of studies exist that permit such comparisons for P_{tot}, field data of size fractionated primary production which are adequate for comparisons with the v1-derived estimates of P_{micro}, P_{nano}, and

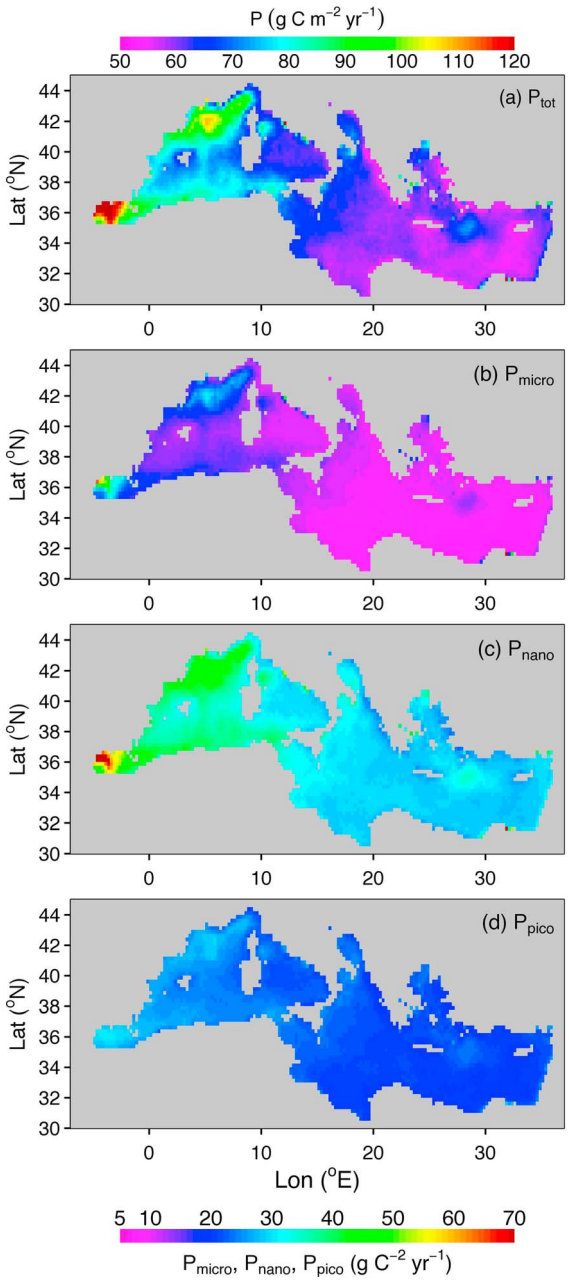

Figure 4. Annual climatological (1998–2007) map of (a) total primary production and (b–d) class-specific primary production (in units of g C m^{-2} yr^{-1}) obtained from the v1 model. Note the two different color scales for the total and class-specific primary production.

P_{pico}, are extremely scarce in the literature. Therefore, in addition to presenting a very limited number of comparisons of our estimates of class-specific primary production with the corresponding estimates based on field measurements available in the literature, we also present comparisons of our estimates of class-specific chlorophyll *a* concentration with field data of size fractionated chlorophyll *a* biomass. The adequate information on size fractionated parameters based on field studies is limited not only because of limited number of size fractionated measurements but also because there often exists a mismatch between the size fractions determined in field experiments and the standard micro, nano, and picophytoplankton size classes involved in our phytoplankton class-specific approach. As a result the size-fractionated field measurements are not always strictly comparable with our v1-derived estimates, so we disregarded such field data from our considerations. Specifically, we compare our model-derived monthly estimates of Chl biomass and primary production associated with the picophytoplankton class with field data from the literature for the <2 μm size fraction. We also compare the model-derived monthly estimates of Chl biomass for the sum of nano and microphytoplankton, microphytoplankton, and in one case nanophytoplankton with field data for the >2 μm, >20 μm, and 2–20 μm size fractions, respectively. For the comparisons involving P_{tot} as well as the class-specific Chl and primary production data, we use the minimum and maximum values of the mean regional v1-derived estimates observed during the full 10 year time series, which characterize the overall range of these estimates. These ranges are compared with the corresponding estimates based on field measurements. It must also be emphasized that the field-based regional estimates are limited in terms of spatial coverage because these estimates are often obtained from measurements made at few locations.

3. Results

[15] Figure 2 illustrates the mean seasonal cycle of total primary production, P_{tot}, obtained from the three different versions of the primary production model for the five selected clusters. First, we consider the results from the v1 model. Overall, the P_{tot} values are low and remain within a relatively limited range of 0.11–0.42 g C m^{-2} d^{-1}. One can observe a regional increase in P_{tot} magnitude and also an increase in seasonal variability from the regions included in the "nonblooming" clusters C1 and C2 to those included in the "blooming" cluster C5. The clusters C1 and C2 (Figures 2a and 2b) show almost identical seasonal cycles of P_{tot} with a primary maximum in June (0.24 g C m^{-2} d^{-1}) and a minimum in December (~0.10 g C m^{-2} d^{-1}). The third "nonblooming" cluster, C3 (Figure 2c), exhibits a primary maximum in July (0.26 g C m^{-2} d^{-1}), a weaker maximum in February (0.23 g C m^{-2} d^{-1}), and minimum values in November (0.14 g C m^{-2} d^{-1}). The "intermittently blooming" cluster, C4 (Figure 2d), displays two maxima of similar magnitude, one in March–April and the other in June–July (~0.27 g C m^{-2} d^{-1}). Finally C5 (Figure 2e) is characterized by a prominent maximum in April (0.42 g C m^{-2} d^{-1}), intermediate values in June–July (0.27 g C m^{-2} d^{-1}), and minimum values in December (0.14 g C m^{-2} d^{-1}).

[16] Both the P_{tot} magnitude and its seasonal pattern show significant differences between the results obtained from the v1 model and the two other versions of the model, v2 and v3, which are included in Figure 2 for comparison. On average, P_{tot} from the v1 model is reduced by a factor of 2.1 (range of 1.6–2.7) and 2.6 (range of 1.8–3.2) compared with the v2 and v3 models, respectively. This reduction factor exhibits significant seasonal changes but limited regional variability. For example, the v1-derived estimates of P_{tot} are lower by a factor of 1.7–2.5 and 1.6–2.6 than the v2-derived estimates for the clusters C1 and C5,

Table 1. Estimates of Mean Annual Total (P_{tot}) and Class-Specific Primary Production (P_{micro}, P_{nano}, and P_{pico}) (in Units of g C m^{-2} yr^{-1}) Obtained From the v1 Model for the Entire Mediterranean Basin, the Five Considered Clusters, and the "Classic" Mediterranean Regions [e.g., see *Bosc et al.*, 2004][a]

	v1 Model				v2 Model,	v3 Model,
	Ptot	Pmicro	Pnano	Ppico	Ptot	Ptot
Mediterranean	68	12 (19%)	33 (48%)	23 (33%)	120	169
C1	63	14 (22%)	29 (46%)	20 (32%)	117	175
C2	63	14 (22%)	29 (46%)	20 (32%)	123	186
C3	72	17 (23%)	33 (46%)	22 (31%)	130	199
C4	71	18 (25%)	32 (45%)	21 (30%)	130	210
C5	78	22 (28%)	35 (45%)	22 (27%)	137	225
Western Basin	79	16 (21%)	38 (48%)	25 (31%)	138	192
Eastern Basin	61	10 (17%)	30 (48%)	21 (35%)	109	156
Adriatic Sea	71	14 (20%)	33 (46%)	24 (34%)	144	200
Alboran Sea	105	26 (25%)	50 (48%)	28 (27%)	174	253
Algerian Basin	78	15 (20%)	37 (48%)	25 (32%)	135	192
Algero-Provençal Basin	78	16 (20%)	37 (48%)	25 (32%)	132	177
Balearic Sea	80	16 (20%)	38 (48%)	26 (32%)	139	192
Aegean Sea	60	10 (17%)	29 (48%)	21 (35%)	119	172
Gulf of Lion	97	24 (25%)	45 (47%)	27 (28%)	170	222
North Ionian Sea	63	11 (17%)	30 (48%)	22 (35%)	115	162
South Ionian Sea	61	10 (16%)	30 (49%)	21 (35%)	103	146
North Levantine Basin	60	10 (16%)	29 (49%)	21 (35%)	105	152
South Levantine Basin	59	10 (17%)	29 (49%)	20 (34%)	103	147
Ligurian Sea	80	19 (23%)	37 (47%)	24 (30%)	147	194
Tyrrhenian Sea	67	12 (18%)	32 (48%)	23 (34%)	122	169

[a]The percent values in parentheses represent the contribution of a given phytoplankton class to P_{tot}. For comparison, the estimates of P_{tot} obtained with the v2 and v3 models are also shown.

respectively. In terms of the seasonal pattern, whereas the v1 model produces a P_{tot} maximum in spring or late winter, and/or in summer depending on the considered cluster, the v2 model always yields only one maximum of P_{tot} in April, whose magnitude increases regionally from C1 (0.45 g C m^{-2} d^{-1}) to C5 (0.67 g C m^{-2} d^{-1}). In contrast, the v3 model produces a distinct summer maximum with P_{tot} varying regionally between 0.63 and 0.81 g C m^{-2} d^{-1}. This model yields a spring maximum only for the cluster C5.

[17] The mean seasonal cycle of class-specific primary production obtained from the v1 model is displayed in Figure 3. For each cluster, the seasonal cycle of primary production associated with nanophytoplankton, P_{nano}, is very similar to that of P_{tot}, which indicates that the variability in P_{tot} is caused largely by P_{nano} (Figures 3a–3e). The relative contributions of micro and picophytoplankton to P_{tot} vary with time and ecological regime. For C1 and C2, most of the seasonal signal of P_{tot} is caused by both P_{nano} and P_{pico} (Figures 3a and 3b). For C3, C4, and C5, the late winter-spring maxima of P_{tot} result from an increase in P_{micro} and P_{nano}, whereas the summer maxima are associated with an increase in P_{nano} and P_{pico} (Figures 3c–3e). In particular for C5, the spring bloom is driven primarily by an increase in P_{micro} by a factor of ~4 compared to the level in January. In contrast to micro and nanophytoplankton whose production maxima are observed in late winter, spring, or summer depending on the cluster, the picophytoplankton production consistently exhibits maxima in summer.

[18] Nanophytoplankton make a dominant contribution (43–50%) to P_{tot} throughout the year in each cluster (Figures 3f–3j). The percent contributions of micro and picophytoplankton exhibit a relatively stable seasonal cycle for C1 and C2 (Figures 3f and 3g) with a larger role of P_{pico} (~32%) than P_{micro} (~22%) (Figures 3f and 3g). These contributions are a little more variable for C3, C4, and C5, with C5 showing the largest temporal dynamics among the five clusters (Figures 3h–3j). The contribution of picophytoplankton typically exceeds that of microphytoplankton most of the year. The exception is observed during a period that coincides with the late winter-spring maximum of P_{tot}, whose start time is delayed and duration increases as one moves from C3 to C4 and C5. For C3, the percent contributions of micro and picophytoplankton are almost the same (~25% each) from January to February. For C4, P_{micro} (27–28% of P_{tot}) slightly exceeds P_{pico} (25–27% of P_{tot}) from February to April. For C5, P_{micro} (27–38% of P_{tot}) is considerably more important than P_{pico} (20–27% of P_{tot}) during a longer time period of February–May.

[19] The annual climatological maps of total and class-specific primary production obtained from the v1 model are shown in Figure 4. The corresponding basin-scale and regional estimates of production are given in Table 1, which also provides results from the v2 and v3 models. With the v1 model, we obtained a mean annual P_{tot} of 68 g C m^{-2} yr^{-1} for the whole Mediterranean basin, with contributions of 19%, 48%, and 33% associated with P_{micro}, P_{nano}, and P_{pico}, respectively. With respect to ecological regimes, the annual P_{tot} increases gradually from cluster C1 (63 g C m^{-2} yr^{-1}) to C5 (78 g C m^{-2} yr^{-1}). The contribution of microphytoplankton to P_{tot} increases within a range of 22–28% from C1 to C5, while that of picophytoplankton decreases within the 32–27% range. The P_{nano} fraction stays relatively constant at ~45%.

[20] Table 1 also provides the mean estimates obtained for the "classic" Mediterranean regions [see *Bosc et al.*, 2004] which are smaller in size than the clusters and, therefore, show larger regional variability in primary production. The

Table 2. Comparison of Annual Rates of Total Phytoplankton Primary Production Estimated From the v1 Model With Those Obtained From Field Measurements (in Units of g C m^{-2} yr^{-1})[a]

References	Area	Period	Field Measurements	This Study (v1)
Sournia [1973]	Whole Basin	Climatology	80–90	65–71
Lefevre et al. [1997]	Gulf of Lion (South)	Climatology	78–142	82–105
Conan et al. [1998]	Gulf of Lion (South)	1993	140–150	82–105
Marty and Chiavérini [2002]	Ligurian Sea (DYFAMED)	1993–99	86–232	72–90
Boldrin et al. [2002]	Adriatic Sea (South)	1997–1999	97.3	66–78
Dugdale and Wilkerson [1988]	Aegean Sea		20.3	54–63
Psarra et al. [2000]	Aegean Sea (Cretan Sea)	Jul 1994–October 1995	59	54–63
Ignatiades [1998]	Aegean Sea (Cretan Sea)	1994	24.79	54–63
Boldrin et al. [2002]	Ionian Sea	1997–1999	61.8	58–67
Dowidar [1984]	South Levantine Basin	1982	55.5	57–62

[a]The reported ranges for the v1-derived values are defined by the minimum and maximum mean regional estimates observed during the 10 year time series.

southern part of the Levantine basin (included in C2) shows the lowest annual P_{tot} of the entire basin (59 g C m^{-2} yr^{-1}), while the Alboran Sea (included in C4) exhibits the highest P_{tot} (105 g C m^{-2} yr^{-1}). The Gulf of Lion, which is part of C5, also shows a relatively high annual rate (97 g C m^{-2} yr^{-1}). For comparison purposes, these estimates are, on average, 1.8 and 2.6 times lower than the estimates obtained with the v2 and v3 models, respectively.

[21] Several ^{14}C-based field measurements of total primary production collected in several open ocean locations in the Mediterranean basin are available in the literature for comparison with the v1-derived P_{tot} estimates [e.g., *Siokou-Frangou et al.*, 2010, and references therein]. Such comparisons are presented in Table 2. The values derived from the v1 model are consistent with those reported by *Lefevre et al.* [1997] for the Gulf of Lion (78–142 g C m^{-2} yr^{-1}), *Psarra et al.* [2000] for the Aegean Sea (59 g C m^{-2} yr^{-1}), *Boldrin et al.* [2002] for the Ionian Sea (62 g C m^{-2} yr^{-1}), and *Dowidar* [1984] for the southern part of the Levantine basin (56 g C m^{-2} yr^{-1}). Some discrepancies between the model-derived values and reported measurements may also be found, but with no consistent trend for lower or higher estimates by the model. For example, whereas the mean annual P_{tot} obtained from the v1 model is lower by 20% than the value reported by *Sournia* [1973] for the whole basin (80–90 g C m^{-2} yr^{-1}) and by 27% than that reported by *Boldrin et al.* [2002] for the south Adriatic Sea (97 g C m^{-2} yr^{-1}), the modeled P_{tot} is higher by a factor of 2.4 than the measurements reported by *Ignatiades* [1998] for the Aegean Sea (25 g C m^{-2} yr^{-1}).

[22] We identified one study from the Tyrrhenian Sea [*Decembrini et al.*, 2009], which includes field data of size fractionated primary production adequate for comparisons with our v1-derived estimates for picophytoplankton (Table 3). The range of v1-derived estimates of P_{pico} compare favorably with field data of the contribution of the <2 μm size fraction to total primary production in summer. In winter the v1-derived estimates are lower by about 60% than the field-based estimates. The comparisons for the class-specific Chl show that the v1-derived estimates overlap with field measurements in all cases with the exception of one from the Levantine Basin (Table 3). In that latter case, the contribution of picophytoplankton to total chlorophyll *a* biomass obtained from the v1 model is lower by about 30% than the field-based estimates for the <2 μm size fraction.

Table 3. Comparison of Phytoplankton Class-Specific Chlorophyll *a* Biomass and Class-Specific Primary Production Estimated From the v1 Model With Field Measurements of Corresponding Size-Fractionated Parameters, Expressed as Percent Contribution of Each Size Class to Total Chlorophyll *a* Biomass (Chl) and Primary Production (P)[a]

			Field Measurements			This Study (v1)		
Reference	Area	Period	Size Class	Chl (%)	P (%)	Size Class	Chl (%)	P (%)
Decembrini et al. [2009]	Tyrrhenian Sea (South)	July 2005	<2 μm	44–81	23–61	Pico	45–46	35–36
		December 2005	<2 μm	76–90	82–94	Pico	41–45	31–36
Morán et al. [2001]	Algerian Basin	October 1996	<2 μm	42–62		Pico	42–46	
			>2 μm	38–58		Nano+Micro	54–58	
Revelante and Gilmartin [1995]	Adriatic Sea (North)	August 1986 and 1988, July 1987	>20 μm	10–23		Micro	13–20	
Arin et al. [2002] and L. Arin, personal communication, 2011	Alboran Sea	May 1998	<2 μm	26–51		Pico	28–41	
			2–20 μm	36–47		Nano	43–46	
			>20 μm	6–35		Micro	16–28	
Arin et al. [2005] and L. Arin, personal communication, 2011	Balearic Sea	February 1997	<2 μm	26–47		Pico	28–38	
			>2 μm	53–74		Micro+Nano	62–72	
		July 1997	<2 μm	26–65		Pico	45–46	
			>2 μm	35–74		Micro+Nano	54–55	
Zohary et al. [1998]	Levantine Basin	March 1992	<2 μm	54.3–64.2		Pico	39–45	

[a]The reported ranges for the v1-derived values are defined by the minimum and maximum mean regional estimates observed during the 10 year time series for the month under consideration.

4. Discussion

[23] The oligotrophic status of the Mediterranean has long been recognized [*Sournia*, 1973] and is supported by our new low estimates of P_{tot} (59–105 g C m^{-2} d^{-1}, Table 1) obtained with the v1 model. These estimates show a general trend of decrease from west to east, which is typically observed in ocean color data of Chl_{surf} [*Bosc et al.*, 2004; *Barale et al.*, 2008]. The ultraoligotrophic and oligotrophic waters dominate the eastern and central parts of the Mediterranean, which are classified as "nonblooming" clusters (C1–C2), and show the lowest P_{tot} of the basin with a maximum in summer. Because algal biomass is very low all year long in these waters, the P_{tot} maximum essentially results from the increase in surface PAR during summer. This maximum is observed despite the fact that the phytoplankton class-specific approach produces a decrease in the overall photosynthetic performance of the phytoplankton community during this season. Although the effect of some model artifact cannot totally be ruled out, the occurrence of the P_{tot} maximum in summer under strong oligotrophic conditions appears reasonable.

[24] In contrast to the nonblooming clusters, the Ligurian Sea and the Gulf of Lion located in the northernmost part of western basin (representing approximately C5) are characterized by the occurrence of an annual spring bloom fueled by nutrient enrichment of the euphotic zone following deep winter mixing. In addition to this pattern, several confined areas of increased productivity are scattered throughout the basin. These waters belong to the "intermittently blooming" regime (C4) and are characterized by complex physical and chemical processes, such as water mass circulation, mesoscale hydrological structures, and allochthonous nutrient inputs, which have the potential of alleviating the general nutrient limitation (e.g., review by *Siokou-Frangou et al.* [2010]). This is observed, for example, in the Alboran Sea, which shows the highest P_{tot} of the entire basin, and the Rhodes Gyre that forms a distinct area of moderate productivity within the ultraoligotrophic northern part of Levantine basin (Figure 4).

[25] The analysis performed by utilizing three different versions of the primary production model revealed dramatic changes in P_{tot} magnitude and seasonal cycle. These changes arise largely from differences in the satellite estimates of Chl_{surf}, which depend on whether or not the chlorophyll algorithm includes the CDOM correction procedure (data not shown). The CDOM correction results in the reduction of Chl_{surf} estimates on average by a factor of 2.5 (range of 1.7–3.1) with consequent decrease of P_{tot}. The effects of the Chl_{surf} estimation on the output of primary production models involve multiple factors. Differences in Chl_{surf} translate not only into changes in vertical profiles of algal biomass with subsequent changes in light propagation and availability for photosynthesis within the water column, but also into modifications of the phytoplankton community composition and associated photophysiological properties.

[26] In the v3 model, the dependence of photophysiology on temperature also comes into play along with the absence of class-specific information about chlorophyll *a* biomass and photophysiology. Whereas the v2 and v3 models provide relatively consistent P_{tot} values in winter, the temperature effect included in v3 combined with high surface PAR largely explains the P_{tot} maximum observed regularly in summer regardless of the cluster under consideration. More specifically, *Morel* [1991] introduced the concept of photosynthetic cross section per unit chlorophyll *a*, Ψ^*, which describes the efficiency of conversion of light available for photosynthesis into chemical energy by the total phytoplankton community within the entire productive layer. In the primary production model, Ψ^* depends on the photophysiological parameters and is also controlled by variations in surface PAR and vertical distribution of chlorophyll *a.* All these factors together determine the light available for photosynthesis at each depth within the productive layer and the consequent status of primary production occurring either under light-limited or light-saturated conditions. These characteristics are common to all three versions of the model and they produce an increase of Ψ^* in winter and a decrease of Ψ^* in summer at temperate latitudes [*Morel*, 1991; *Antoine et al.*, 1995; *Antoine and Morel*, 1996]. In the v3 model, this effect is somewhat counterbalanced by high summer temperatures that tend to increase Ψ^* and promote primary production. In contrast, the phytoplankton class-specific approach (v1 and v2) modulates Ψ^* through changes in phytoplankton community composition. In summer, low Chl_{surf} values are associated with decreased contributions of microphytoplankton population, which is more efficient photosynthetically than smaller cells, and increased contributions of picophytoplankton with lower photosynthetic efficiency. This results in relatively low P_{tot} values in summer despite the surface PAR maximum. Whereas the temperature-based parameterization (as included in v3) has been questioned in the past [*Morel*, 1991; *Antoine et al.*, 1995; *Bricaud et al.*, 2002], the present analysis supports the phytoplankton class-specific approach in which the community composition is driven by the main environmental factors (such as irradiance, nutrients, temperature) that modulate algal photophysiological response [*Bouman et al.*, 2005; *Claustre et al.*, 2005]. This approach thus implies that the community composition is a reasonable indicator of algal photophysiology.

[27] The phytoplankton class-specific approach utilized in this study shows that the basin-scale P_{tot} in the Mediterranean can be more than two times lower than previously estimated from ocean color data obtained with standard [*Antoine et al.*, 1995] or regional [*Bosc et al.*, 2004] algorithms. This result clearly points to the necessity of pursuing the refinement of ocean color Chl_{surf} algorithms. In addition, this approach also indicates that primary production is dominated by nanophytoplankton throughout the year and entire basin. Under oligotrophic "nonblooming" conditions, picophytoplankton dominate in terms of biomass, but nanophytoplankton are characterized by superior photosynthetic performances. In moderate bloom conditions, an increase in algal biomass is associated primarily with nanophytoplankton. As expected, microphytoplankton (essentially diatoms) clearly dominate over picophytoplankton during blooms, whereas picophytoplankton outgrow diatoms in the most oligotrophic conditions. Although the observed nanophytoplankton ubiquity might be surprising at first, it is in agreement with several reports of phytoplankton pigment and size-fractionated chlorophyll *a* data indicating the

significance of this group in both oligotrophic and bloom conditions within the Mediterranean basin [*Vidussi et al.*, 2001; *Arin et al.*, 2002; *Psarra et al.*, 2005; *Marty et al.*, 2008]. We note, however, that some studies also report a dominant contribution of pico-sized cells to algal biomass and primary production in the Mediterranean [*Magazzù and Decembrini*, 1995], which suggests that the v1 model might underestimate P_{pico} on some occasions.

[28] Considering the multiple sources of differences between the field measurement approaches and the modeling approaches involving remote sensing data (e.g., mismatch of space-time scales, thickness of the water column considered for integration of production values), the reasonable agreement found between the field measurements and our estimates from the v1 model is encouraging (Table 2). We also note that the total primary production resulting from our phytoplankton class-specific approach has been evaluated satisfactorily against in situ data from the Mediterranean Sea as part of round-robin experiment focused on total primary production algorithms [*Saba et al.*, 2011].

[29] In terms of phytoplankton class-specific Chl and primary production, the comparative analysis presented in this study shows generally good agreement between the ranges of v1-derived estimates and field data (Table 3). However, this analysis must be considered with appropriate caution merely as a first preliminary step toward more rigorous validation of satellite-based model estimates of class-specific data products against field measurements. The rigorous validation is a complex problem. The difficulties arise primarily from the lack of appropriate size-fractionated data from field experiments as well as inconsistencies between the size-fractionated data from field determinations and the standard micro, nano, and picophytoplankton size classes [*Sieburth et al.*, 1978] nominally assigned to the pigment-based classes involved in the modeling approach. Therefore, at the present time the rigorous validation of satellite-derived estimates of phytoplankton class-specific Chl and primary production in the Mediterranean Sea appears impossible. It would require assembling a comprehensive matchup data set consisting of concurrent field measurements and satellite-derived values of Chl_{surf}, size-fractionated Chl, as well as total and size-fractionated primary production. Such a data set would have to satisfy quite stringent requirements of proximity in both space and time between the field determinations and satellite overpassess, which are recommended for this type of validation studies [*Bailey and Werdell*, 2006].

[30] Whereas we recognize that the rigorous validation studies of phytoplankton class-specific data products derived from the combination of remote sensing and modeling represents an important task for future efforts, the present study highlights the first ocean color–derived estimates of primary production associated with three major phytoplankton types along with a reevaluation of total primary production in the Mediterranean Sea over the past decade. In contrast to previous ocean color–based studies that focused on algal biomass as a single component, we address the role of the composition of phytoplankton communities at a quantitative level in terms of primary production. This is an essential advancement considering the role of phytoplankton biodiversity as a major driver of oceanic carbon cycling [e.g., *Kiørboe*, 1993; *Guidi et al.*, 2009]. Furthermore, the proposed climatological (10 year) mean data of class-specific and total primary production represent an important reference for future studies on the responses of pelagic ecosystems to environmental changes and associated biogeochemical variability in the Mediterranean.

[31] **Acknowledgments.** This research was supported by the NASA Biodiversity Program (grant NNX09AK17G) and by the SESAME (Southern European Seas: Assessing and Modeling Ecosystem Changes) project (EC contract GOCE-036949) funded by the European Commission's Sixth Framework Program. The authors wish to thank the SeaWiFS Project and the NASA Distributed Active Archive Center at the Goddard Space Flight Center for the production and distribution of the SeaWiFS data. We acknowledge Laura Arin for kindly making available field data of size-fractionated chlorophyll *a* biomass. We also thank two anonymous reviewers for helpful comments on the manuscript.

References

Antoine, D., and A. Morel (1996), Oceanic primary production: 1. Adaptation of a spectral light-photosynthesis model in view of application to satellite chlorophyll observations, *Global Biogeochem. Cycles*, *10*, 43–55, doi:10.1029/95GB02831.

Antoine, D., A. Morel, and J.-M. André (1995), Algal pigment distribution and primary production in the eastern Mediterranean as derived from coastal zone color scanner observations, *J. Geophys. Res.*, *100*, 16,193–16,209, doi:10.1029/95JC00466.

Arin, L., X. A. G. Morán, and M. Estrada (2002), Phytoplankton size distribution and growth rates in the Alboran Sea (SW Mediterranean): Short term variability related to mesoscale hydrodynamics, *J. Plankton Res.*, *24*, 1019–1033, doi:10.1093/plankt/24.10.1019.

Arin, L., M. Estrada, J. Salat, and A. Cruzado (2005), Spatio-temporal variability of size fractionated phytoplankton on the shelf adjacent to the Ebro river (NW Mediterranean), *Cont. Shelf Res.*, *25*, 1081–1095, doi:10.1016/j.csr.2004.12.011.

Bailey, S. W., and P. J. Werdell (2006), A multi-sensor approach for the on-orbit validation of ocean color satellite data products, *Remote Sens. Environ.*, *102*, 12–23, doi:10.1016/j.rse.2006.01.015.

Barale, V., J.-M. Jaquet, and M. Ndiaye (2008), Algal blooming patterns and anomalies in the Mediterranean Sea as derived from the SeaWiFS data set (1998–2003), *Remote Sens. Environ.*, *112*, 3300–3313, doi:10.1016/j.rse.2007.10.014.

Bethoux, J. P., B. Gentili, P. Morin, E. Nicolas, C. Pierre, and D. Ruiz-Pino (1999), The Mediterranean Sea: A miniature ocean for climatic and environmental studies and a key for the climatic functioning of the North Atlantic, *Prog. Oceanogr.*, *44*, 131–146, doi:10.1016/S0079-6611(99)00023-3.

Boldrin, A., S. Miserocchi, S. Rabitti, M. M. Turchetto, V. Balboni, and G. Socal (2002), Particulate matter in the southern Adriatic and Ionian Sea: Characterisation and downward fluxes, *J. Mar. Syst.*, *33–34*, 389–410, doi:10.1016/S0924-7963(02)00068-4.

Bosc, E., A. Bricaud, and D. Antoine (2004), Seasonal and interannual variability in algal biomass and primary production in the Mediterranean Sea, as derived from 4 years of SeaWiFS observations, *Global Biogeochem. Cycles*, *18*, GB1005, doi:10.1029/2003GB002034.

Bouman, H., T. Platt, S. Sathyendranath, and V. Stuart (2005), Dependence of light-saturated photosynthesis on temperature and community structure, *Deep Sea Res., Part I*, *52*, 1284–1299, doi:10.1016/j.dsr.2005.01.008.

Brewin, R. J. W., N. J. Hardman-Mountford, S. J. Lavender, D. E. Raitsos, T. Hirata, J. Uitz, E. Devred, A. Bricaud, A. Ciotti, and B. Gentili (2011), An intercomparison of bio-optical techniques for detecting dominant phytoplankton size class from satellite remote sensing, *Remote Sens. Environ.*, *115*, 325–339, doi:10.1016/j.rse.2010.09.004.

Bricaud, A., E. Bosc, and D. Antoine (2002), Algal biomass and sea surface temperature in the Mediterranean Basin: Intercomparison of data from various satellite sensors, and implications for primary production estimates, *Remote Sens. Environ.*, *81*, 163–178, doi:10.1016/S0034-4257(01)00335-2.

Bricaud, A., H. Claustre, J. Ras, and K. Oubelkheir (2004), Natural variability of phytoplanktonic absorption in oceanic waters: Influence of the size structure of algal populations, *J. Geophys. Res.*, *109*, C11010, doi:10.1029/2004JC002419.

Claustre, H., A. Morel, S. B. Hooker, M. Babin, D. Antoine, K. Oubelkheir, A. Bricaud, K. Leblanc, B. Quéguiner, and S. Maritorena (2002), Is desert dust making oligotrophic waters greener?, *Geophys. Res. Lett.*, *29*(10), 1469, doi:10.1029/2001GL014056.

Claustre, H., M. Babin, D. Merien, J. Ras, L. Prieur, S. Dallot, O. Prasil, H. Dousova, and T. Moutin (2005), Toward a taxon-specific parameterization of bio-optical models of primary production: A case study in the North Atlantic, *J. Geophys. Res.*, *110*, C07S12, doi:10.1029/2004JC002634.

Conan, P., M. Pujo-Pay, P. Raimbault, and M. Leveau (1998), Hydrological and biological variability in the Gulf of Lions. II. Productivity on the inner edge of the North Mediterranean current, *Oceanol. Acta*, *21*, 767–782, doi:10.1016/S0399-1784(99)80005-X.

Decembrini, F., C. Caroppo, and M. Azzaro (2009), Size structure and production of phytoplankton community and carbon pathways channeling in the southern Tyrrhenian Sea (western Mediterranean), *Deep Sea Res., Part II*, *56*, 687–699, doi:10.1016/j.dsr2.2008.07.022.

D'Ortenzio, F., and M. Ribera d'Alcalà (2009), On the trophic regimes of the Mediterranean Sea: A satellite analysis, *Biogeosciences*, *6*, 139–148, doi:10.5194/bg-6-139-2009.

D'Ortenzio, F., S. Marullo, M. Ragni, M. Ribera D'Alcalà, and R. Santoleri (2002), Validation of empirical SeaWiFS algorithms for chlorophyll-*a* retrieval in the Mediterranean Sea. A case study for oligotrophic seas, *Remote Sens. Environ.*, *82*, 79–94, doi:10.1016/S0034-4257(02)00026-3.

D'Ortenzio, F., D. Iudicone, C. de Boyer Montegut, D. Antoine, S. Marullo, R. Santoleri, and G. Madec (2005), Seasonal variability of the mixed layer depth in the Mediterranean Sea as derived from in situ profiles, *Geophys. Res. Lett.*, *32*, L12605, doi:10.1029/2005GL022463.

Dowidar, N. M. (1984), Phytoplankton biomass and primary productivity of the south-eastern Mediterranean, *Deep Sea Res., Part A*, *31*, 983–1000, doi:10.1016/0198-0149(84)90052-9.

Dugdale, R. C., and F. P. Wilkerson (1988), Nutrient sources and primary production in the eastern Mediterranean, *Oceanol. Acta*, *9*, 179–184.

Eppley, R. W. (1972), Temperature and phytoplankton growth in the sea, *Fish. Bull.*, *70*, 1063–1085.

Giorgi, F. (2006), Climate change hot-spots, *Geophys. Res. Lett.*, *33*, L08707, doi:10.1029/2006GL025734.

Gregg, W. W., and N. W. Casey (2004), Global and regional evaluation of the SeaWiFS chlorophyll data set, *Remote Sens. Environ.*, *93*, 463–479, doi:10.1016/j.rse.2003.12.012.

Guidi, L., L. Stemmann, G. A. Jackson, F. Ibanez, H. Claustre, L. Legendre, M. Picheral, and G. Gorsky (2009), Effects of phytoplankton community on production, size, and export of large aggregates: A world-ocean analysis, *Limnol. Oceanogr.*, *54*, 1951–1963, doi:10.4319/lo.2009.54.6.1951.

Ignatiades, L. (1998), The productive and optical status of the oligotrophic waters of the southern Aegean Sea (Cretan Sea), eastern Mediterranean, *J. Plankton Res.*, *20*, 985–995, doi:10.1093/plankt/20.5.985.

Kiørboe, T. (1993), Turbulence, phytoplankton cell size, and the structure of pelagic food webs, *Adv. Mar. Biol.*, *29*, 1–72, doi:10.1016/S0065-2881(08)60129-7.

Lazzara, L., C. Marchese, L. Massi, C. Nuccio, F. Maselli, C. Santini, M. Pieri, and V. Sorani (2010), Sub-regional patterns of primary production annual cycle in the Ligurian and North Tyrrhenian Seas, from satellite data, *Ital. J. Remote Sens.*, *42*, 87–102, doi:10.5721/ItJRS20104227.

Lefevre, D., H. J. Minas, M. Minas, C. Robinson, P. J. L. B. Williams, and E. M. S. Woodward (1997), Review of gross community production, primary production, net community production and dark community respiration in the Gulf of Lions, *Deep Sea Res., Part II*, *44*, 801–819, 821–832, doi:10.1016/S0967-0645(96)00091-4.

Magazzù, G., and F. Decembrini (1995), Primary production, biomass and abundance of phototrophic picoplankton in the Mediterranean Sea: A review, *Aquat. Microb. Ecol.*, *9*, 97–104, doi:10.3354/ame009097.

Marty, J.-C., and J. Chiavérini (2002), Seasonal and interannual variations in phytoplankton production at DYFAMED time-series station, northwestern Mediterranean Sea, *Deep Sea Res., Part II*, *49*, 2017–2030, doi:10.1016/S0967-0645(02)00025-5.

Marty, J.-C., N. Garcia, and P. Raimbault (2008), Phytoplankton dynamics and primary production under late summer conditions in the NW Mediterranean Sea, *Deep Sea Res., Part I*, *55*, 1131–1149, doi:10.1016/j.dsr.2008.05.001.

Morán, X. A. G., I. Taupier-Letage, E. Vázquez-Domínguez, S. Ruiz, L. Arin, P. Raimbault, and M. Estrada (2001), Physical-biological coupling in the Algerian Basin (SW Mediterranean): Influence of mesoscale instabilities on the biomass and production of phytoplankton and bacterioplankton, *Deep Sea Res., Part I*, *48*, 405–437, doi:10.1016/S0967-0637(00)00042-X.

Morel, A. (1991), Light and marine photosynthesis: A spectral model with geochemical and climatological implications, *Prog. Oceanogr.*, *26*, 263–306, doi:10.1016/0079-6611(91)90004-6.

Morel, A., and J.-M. André (1991), Pigment distribution and primary production in the western Mediterranean as derived and modeled from coastal zone color scanner observations, *J. Geophys. Res.*, *96*, 12,685–12,698, doi:10.1029/91JC00788.

Morel, A., and B. Gentili (2009a), A simple band ratio technique to quantify the colored dissolved and detrital organic material from ocean color remotely sensed data, *Remote Sens. Environ.*, *113*, 998–1011, doi:10.1016/j.rse.2009.01.008.

Morel, A., and B. Gentili (2009b), The dissolved yellow substance and the shades of blue in the Mediterranean Sea, *Biogeosciences*, *6*, 2625–2636, doi:10.5194/bg-6-2625-2009.

Nair, A., S. Sathyendranath, T. Platt, J. Morales, V. Stuart, M.-H. Forget, E. Devred, and H. Bouman (2008), Remote sensing of phytoplankton functional types, *Remote Sens. Environ.*, *112*, 3366–3375, doi:10.1016/j.rse.2008.01.021.

O'Reilly, J. E., et al. (2000), Ocean color chlorophyll *a* algorithms for SeaWiFS, OC2, and OC4: Version 4, in *SeaWiFS Postlaunch Calibration and Validation Analyses, Part 3*, *SeaWiFS Postlaunch Tech. Rep. Ser.*, vol. 11, edited by S. B. Hooker and E. R. Firestone, pp. 9–23, NASA Goddard Space Flight Cent., Greenbelt, Md.

Psarra, S., A. Tselepides, and L. Ignatiades (2000), Primary productivity in the oligotrophic Cretan Sea (NE Mediterranean): Seasonal and interannual variability, *Prog. Oceanogr.*, *46*, 187–204, doi:10.1016/S0079-6611(00)00018-5.

Psarra, S., T. Zohary, M. D. Krom, R. F. C. Mantoura, T. Polychronaki, N. Stambler, T. Tanaka, A. Tselepides, and T. F. Thingstad (2005), Phytoplankton response to a Lagrangian phosphate addition in the Levantine Sea (eastern Mediterranean), *Deep Sea Res., Part II*, *52*, 2944–2960, doi:10.1016/j.dsr2.2005.08.015.

Revelante, N., and M. Gilmartin (1995), The relative increase of larger phytoplankton in a subsurface chlorophyll maximum of the northern Adriatic Sea, *J. Plankton Res.*, *17*, 1535–1562, doi:10.1093/plankt/17.7.1535.

Saba, V. S., et al. (2011), An evaluation of ocean color model estimates of marine primary productivity in coastal and pelagic regions across the globe, *Biogeosciences*, *8*, 489–503, doi:10.5194/bg-8-489-2011.

Sieburth, J. McN., V. Smetacek, and J. Lenz (1978), Pelagic ecosystem structure: Heterotrophic compartments of the plankton and their relationship to plankton size fractions, *Limnol. Oceanogr.*, *23*, 1256–1263, doi:10.4319/lo.1978.23.6.1256.

Siokou-Frangou, I., U. Christaki, M. G. Mazzocchi, M. Montresor, M. Ribera d'Alcalá, D. Vaqué, and A. Zingone (2010), Plankton in the open Mediterranean Sea: A review, *Biogeosciences*, *7*, 1543–1586, doi:10.5194/bg-7-1543-2010.

Sournia, A. (1973), *La Production Primaire Planctonique en Méditerranée; Essai de Mise à Jour, Cybium, Nouv. Ser.*, vol. 81, 128 pp., Coop. Invest. in the Mediter., Monte Carlo, Monaco.

The MerMex Group (2011), Marine ecosystems' responses to climatic and anthropogenic forcings in the Mediterranean, *Prog. Oceanogr.*, *91*, 97–166, doi:10.1016/j.pocean.2011.02.003.

Uitz, J., H. Claustre, A. Morel, and S. B. Hooker (2006), Vertical distribution of phytoplankton communities in open ocean: An assessment based on surface chlorophyll, *J. Geophys. Res.*, *111*, C08005, doi:10.1029/2005JC003207.

Uitz, J., Y. Huot, F. Bruyant, M. Babin, and H. Claustre (2008), Relating phytoplankton photophysiological properties to community structure on large scales, *Limnol. Oceanogr.*, *53*, 614–630, doi:10.4319/lo.2008.53.2.0614.

Uitz, J., H. Claustre, F. B. Griffiths, J. Ras, N. Garcia, and V. Sandroni (2009), A phytoplankton class-specific primary production model applied to the Kerguelen Islands region (Southern Ocean), *Deep Sea Res., Part I*, *56*, 541–560, doi:10.1016/j.dsr.2008.11.006.

Uitz, J., H. Claustre, B. Gentili, and D. Stramski (2010), Phytoplankton class-specific primary production in the world's oceans: Seasonal and interannual variability from satellite observations, *Global Biogeochem. Cycles*, *24*, GB3016, doi:10.1029/2009GB003680.

Vidussi, F., H. Claustre, B. B. Manca, A. Luchetta, and J.-C. Marty (2001), Phytoplankton pigment distribution in relation to upper thermocline circulation in the eastern Mediterranean Sea during winter, *J. Geophys. Res.*, *106*, 19,939–19,956, doi:10.1029/1999JC000308.

Volpe, G., R. Santoleri, V. Vellucci, M. Ribera d'Alcalà, S. Marullo, and F. D'Ortenzio (2007), The colour of the Mediterranean Sea: Global versus regional bio-optical algorithms evaluation and implication for satellite chlorophyll estimates, *Remote Sens. Environ.*, *107*, 625–638, doi:10.1016/j.rse.2006.10.017.

Zohary, T., S. Brenner, M. D. Krom, D. L. Angel, N. Kress, W. K. W. Li, A. Neori, and Y. Z. Yacobi (1998), Buildup of microbial biomass during deep winter mixing in a Mediterranean warm-core eddy, *Mar. Ecol. Prog. Ser.*, *167*, 47–57, doi:10.3354/meps167047.